Ahmed Khaled Mohamed Khaled. International Journal of Engineering Research and Applications
www.ijera.com
ISSN: 2248-9622, Vol. 14, Issue 3, March, 2024, pp: 46-57

RESEARCH ARTICLE OPEN ACCESS

Effect of size, shape and distribution of surface defects on the forming of aluminum sheet

Eng. Ahmed Khaled Mohamed Khaled

Abstract
The research was conducted on samples of aluminum sheet with 1 mm thickness, annealed at (275 C°). To examine the effect of the size of surface defects on the stretch forming by introducing defects of different sizes on the surface of the sheet before forming process .Then forming the samples using a hemispherical punch without lubrication up to the fracture point. It was found that the defects size have a big effect on the fracture initiation and its propagation. The same result was found for the defect shape. Also the defect distribution was studied, where the defects distribution shows big effect on fracture position, which gave a clear picture of the forming is concentrated. Giving the opportunity to control forming and reduce the fracture.
Keywords: Aluminum, Stretch forming, Surface defects.
Lo : The length scale of the model before inspection.
L: The length scale of the model after inspection.
F:Applied Force (Newton).
Ao : Model Cross sectional area(mm^2).
σ:True stress .
K: strength coefficient.
ε: true strain.
n : strain hardening exponent.

Date of Submission: 02-03-2024 Date of acceptance: 12-03-2024

I. Introduction:

Cracks are considered a cause for the fracturing of solid materials. When a material is subjected to stress, the atomic bonds elongate, storing elastic energy in the material as a result. This elastic behavior leads to the familiar linear relationship between stress and strain, where the bonds stretch by about 10 – 20% of their original lengths before breaking. While this elastic behavior includes a high resistance against material buckling, in reality, the material never actually reaches this limit. Instead, small existing flaws in the material amplify under localized stress until they become large enough to break the atomic bonds, allowing for the growth of cracks. This behavior, surprisingly universal across different materials, falls into just one of three categories depending on the method of stress application and the form. Figure (1) illustrates this, where mode (i) shows the fracture occurring due to intense load perpendicular to the crack, the most common type of loading in experimental crack studies. Mode (ii) involves surfaces sliding over each other, observed in earthquakes and other frictional processes. A simple example of mode (iii) loading is attempting to tear open a candy wrapper, which would be difficult without the presence of a small initiating crack acting as a seed for further cracking. Modes (i and ii) apply to bulk metal forming, whereas mode (iii) applies to other cases.

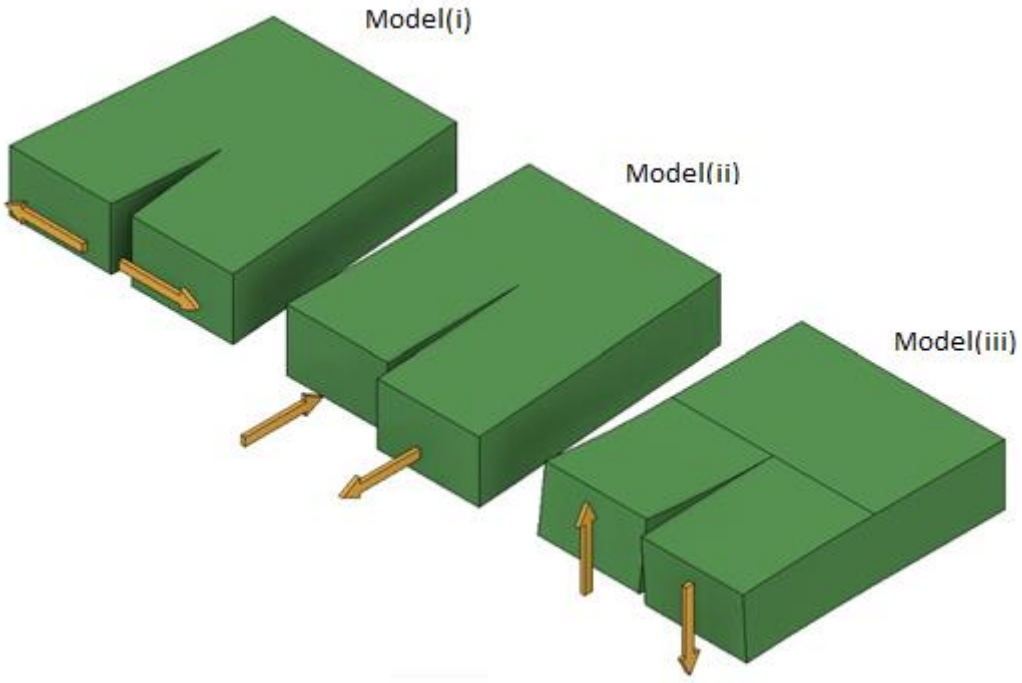

Figure (1) mathematically describe cracks.

Theoretical Part:

In 1920, a British engineer(Alan Griffith) in 1920 used the modes shown in Figure (1) to mathematically describe cracks. He noted that the energy required for the growth of an existing crack is provided by the release of stored elastic energy around the crack. He explained that for short crack lengths, the released elastic energy is less than what is required to break the atomic bonds, suggesting the existence of a critical length that must be exceeded for the crack to continue growing. In reality, if this were not the case, all solid materials would immediately fracture upon being subjected to Tension. To use this theory in studying the onset and growth of fractures in forming processes, it is essential[1] to understand that a metal's formability is a direct result of the interplay of several variables, most importantly the metal's mechanical properties, the forming system used in manufacturing parts, and the lubrication processes employed in that operation. The strain hardening exponent expresses the degree of forming or deformation of the sheet, and strain is typically measured with tools like strain gauges. The strain resulting from tensile stress can be mathematically expressed with the following equation[1&2]:

e=L-L°/L°

……
…..(1)

This strain is referred to as engineering strain .However, the strain referred to as the true strain is calculated from the following equation:

$$\varepsilon \equiv \ln\ (1 + e)$$

……..(2)

The engineering stress (applied load on the specimen under load) can be mathematically expressed: -

S=F/AO

……..(3)

The strain hardening coefficient holds significant importance in metal forming as it provides a clear understanding of the material behavior in the region of uniform deformation, which lies between the yield point and the ultimate tensile strength in the stress-strain engineering diagram. Researchers (K. Sieger & S. Wanger) pointed out that increasing the strain hardening value and the uniform stress decreases the likelihood of local necking and fracture occurrence in the forming process, thereby allowing greater control over the deformation zone of the workpiece and consequently enhancing formability. However, determining the value of the strain hardening coefficient makes it difficult to use engineering stress due to its reliance on a constant cross-sectional area during load application. Therefore, it is necessary to consider the change in the cross-sectional area of the specimen during tensile testing to determine the true stress[4] from the following equation.

σ = S(1+e)

……..(4)

And (n) is calculated from the following equation.

$\sigma = K \varepsilon^{\wedge} n$) ……..(5)

The cold forming process, such as rolling, drawing, and extrusion, is typically performed on metals and alloys previously shaped in the hot state and usually represents the final stage of production processes. The effect of cold forming lies in breaking down the crystal structure, causing it to take on a longitudinal shape in the direction of deformation, thereby increasing hardness and reducing ductility, resulting in strain hardening. This is attributed to the significant role played by dislocations during this process, which increase in density thousands of times more than before the start of forming. Therefore, before continuing with various forming operations on cold-worked metals (such as sheets), metal annealing becomes necessary. This is achieved by conducting an annealing process involving reheating the metal to temperatures sufficient to induce structural changes, followed by slow cooling in the furnace[2&5].

II. Materials and Methods:

The practical part of the research includes preparing aluminum sheets and cutting test specimens, conducting heat treatments for the specimens, as well as creating industrial defects for the specimens using various shapes, positions, and methods of distributing these defects. Initially, cold-pressed models were manufactured from 1 mm thick sheets with dimensions of (100*100) *mm* in the mechanical workshop, along with the production of tensile test models according to standard specifications. Subsequently, annealing was carried out for all models, followed by the introduction of various defects on the forming models with a press to determine the effect of the location and shape of these defects on fracture initiation and formation, and thus on formability.

Primary Material Preparation:

The preparation included obtaining a pure aluminum sheet with dimensions of (2000*1000) *mm* and a thickness of (1) *mm*. A sample was taken from the sheet for examination to determine the purity ratio of the aluminum in the sheet, where it was found that the aluminum purity ratio in the sheet is (99.5%) with impurities at a ratio of (0.5%).

Preparation of Test Models:

1- Tensile Test Models: Tensile test models were prepared according to standard specifications (ASTM370), and Figure (2) shows the dimensions of the tensile test model.

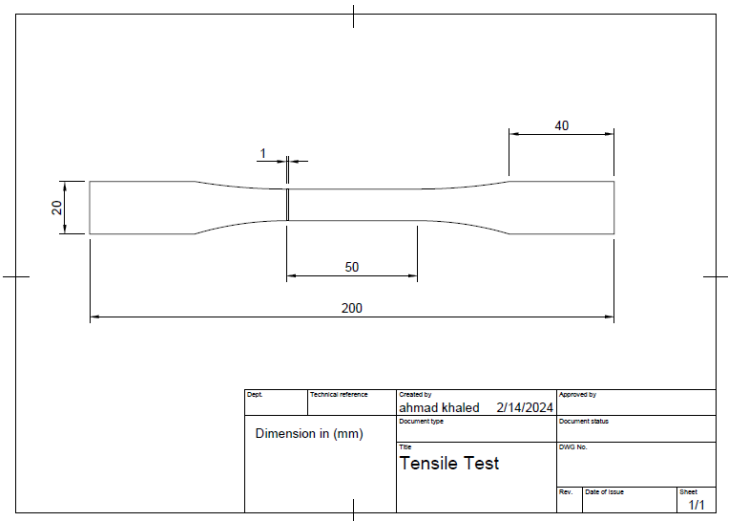

Figure (2): Tensile Test Model According to Standard Specifications

2- Cold Forming Test Models: Models with dimensions of (100*100 *mm*) were manufactured, with a total of (40) pieces produced.

Heat Treatments (Annealing Process):

The stress relief annealing process for the models was carried out using an Electric Muffle Furnace, with a temperature of (275) degrees Celsius selected and a duration of (10 minutes) for the annealing process for the models, based on the aluminum recrystallization temperature. Figure (3) illustrates the stages of the annealing process used in this study.

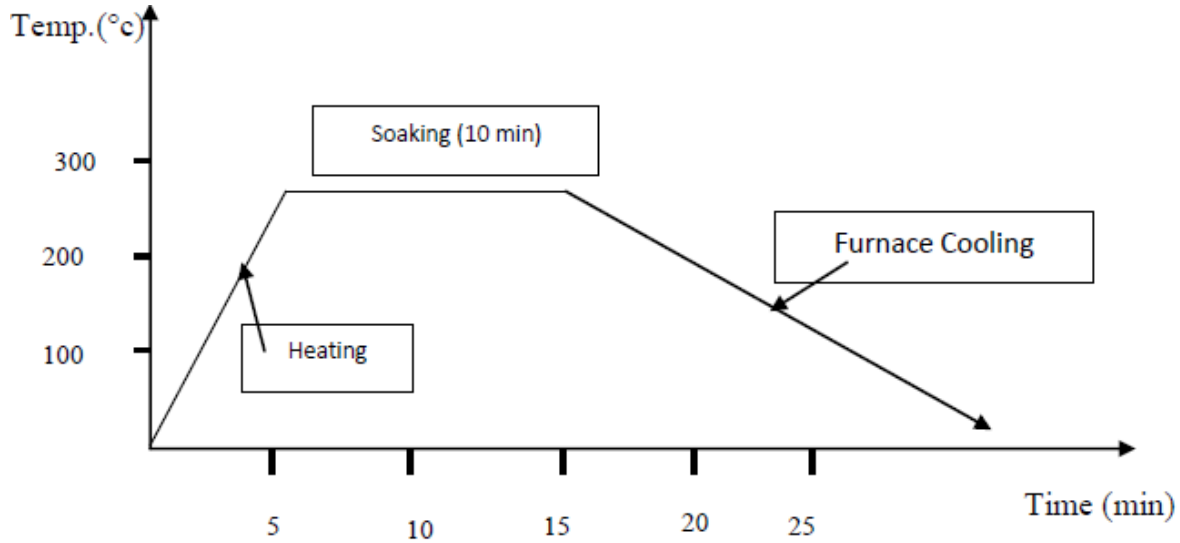

Figure (3): Stages of the Annealing Process.

Selection of External Defects' Location and Shape:

1- Preparation of Models for Studying the Effect of Size and Shape of Defects: For the purpose of studying the effect of defect shape and size, three cases were selected:

A. Cone-shaped defect, where a hardness testing device (using the HRC method) was used to obtain this type of surface defects, with a defect size of (0.025 *mm*), where the cone height = 0.2 *mm*, at an angle of 120 degrees, and with a diameter of the imprint of 0.692 mm.

V = 1/3 HA ……..(6)

B. Hemispherical defect with a diameter of (1.26 *mm*) or a size of (1.047 *mm*), where a hardness testing device using the HRB method was used to obtain this type of surface defects.

V = 4/3 πr^3 ……..(7)

C. Hemispherical defect with a diameter of (1.65 *mm*) or a size of (2.35 *mm*), where iron chisels were manually used to obtain this type of surface defects.

V = 4/3 πr^3 ……..(8)

The depth of the imprint was measured using a Dial gauge, which was attached to the hardness testing device to ensure that all defects have equal depth, and regarding the imprint diameter, it was measured using a microscope with a special calibrated lens for this purpose. Separating the effect of defect shape from its size is a difficult process, and due to the lack of necessary resources for this, dealing with defect shape and sizes was treated as a single factor. To study the effect of defect size and shape on fracture, the other factor, which is the test location, must be fixed. Figure (4) represents some locations with defect distribution methods used. After selecting a fixed location and distribution for defects for all pieces, the shape and size of defects were changed according to the aforementioned three cases, and the forming process was carried out until the tested models fractured.

Figure (4): Illustrates Locations with Defect Distribution Methods Used

2- Preparation of Models for Studying the Effect of Defect Location and Distribution:

For the purpose of studying the effect of defect location and distribution on fracture, the factor (defect shape and size) was fixed. The third type of defects was chosen (hemispherical defect with a diameter of 1.65 *mm*) for all pieces to be examined, as it has the greatest impact, as will be observed from the results.

To understand the effect of defect location and distribution on fracture, different distances from the center of the piece were selected in variable circular shapes(12,16,20,24,24,28,32,36,40,44,48 *mm*). For the effect of defect distribution, two types of distributions were selected:

A. Defect distribution along the periphery of the drawn circles, symbolized by "O" for this distribution.

B. Defect distribution along the diameters perpendicular to the drawn circles, symbolized by "X" for this distribution. As shown in Figure (4).

The metal forming test.:

Forming is one of the important and fundamental processes supporting the metal sheet forming operations. It utilizes a mold, a die, and a half-spherical punch. The metal sheet (model) is placed on the mold, and then the punch is pressed, meaning the material is formed over the punch, taking the shape of the punch, as shown in Figures (5) [6]

The forming process was carried out on the models using a half-spherical punch with the tensile testing device after its conversion into a pressing device, as shown in Figure (7). The model is placed on the mold and firmly secured inside it. The parts (punch, mold, and material holder) are placed on the tensile testing device. Then, the forming of the models is initiated by the punch into the mold at a rate of (20 *mm/min*). The gradual increase in the applied load with the depth of forming is observed until it reaches the maximum limit. When the load decreases, the punch is stopped, as the model may have experienced thinning or fracture. Changes in the models after forming are observed, as shown in Figure (6).

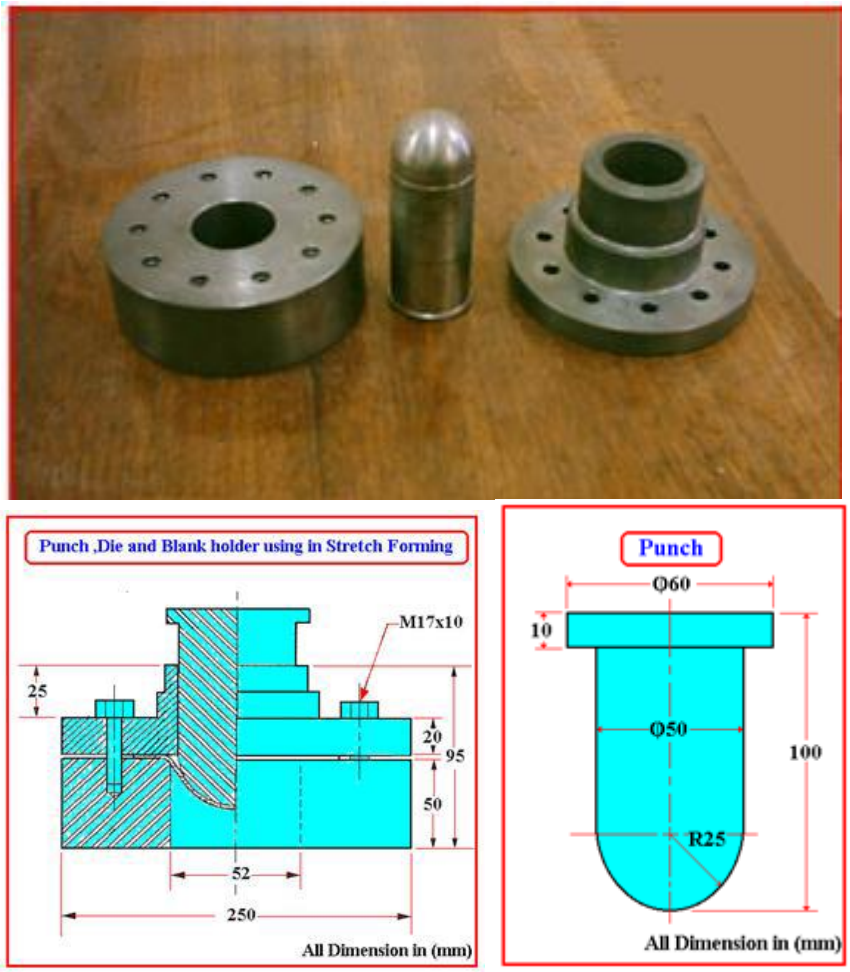

Figure (5): Punch, Mold, and Holder.

Figure (6): Models after Pressing.

Tensile Test:

Tensile tests were conducted using a Wolpert-type tensile testing machine, and the models were manufactured according to the American standard (ASTM370). Figure (7) illustrates the device used in the test.

Fig (7) Tensile testing machine.

III. Results:

Due to the importance of the strain-hardening coefficient (n-value) in the metal sheet forming process, which is considered an important indicator of formability, the value of the strain-hardening coefficient (n-value) was calculated by conducting tensile tests on a sheet metal model. The focus of the test is on the uniform strain region. During the tensile test, an engineering stress-strain plot is created, followed by the creation of true stress-strain plots in the second stage. Through a logarithmic true stress-strain plot, values of (K) and (n) can be found, where (n) represents the slope of the uniform deformation region in the plot, and (K) represents the intersection point (Log ε) at a strain equal to one unit with the linear relationship, with its units representing stress units. This is done using the following equations:

$\sigma = K \varepsilon^n$ ……..(9)
$\text{Log } \sigma = \text{Log } K + \text{Log } \varepsilon$ ……..(10)
If log K = 0
$n = \text{Log } \sigma / \text{Log } \varepsilon$ ……..(11)
at $\varepsilon = 1$
$\text{Log } \varepsilon = 0$
$\text{Log } \sigma = \text{Log } K$
Ao=12.5 mm^2 / Lo =50mm / n=0.25 / k= 302.4 Mpa

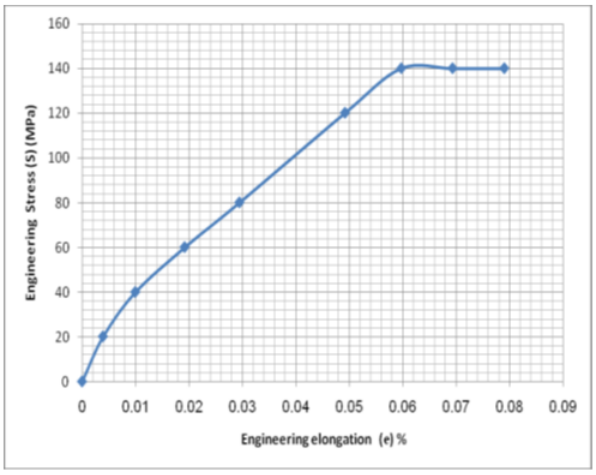

Figure (8): Plot showing the relationship between engineering stress-strain

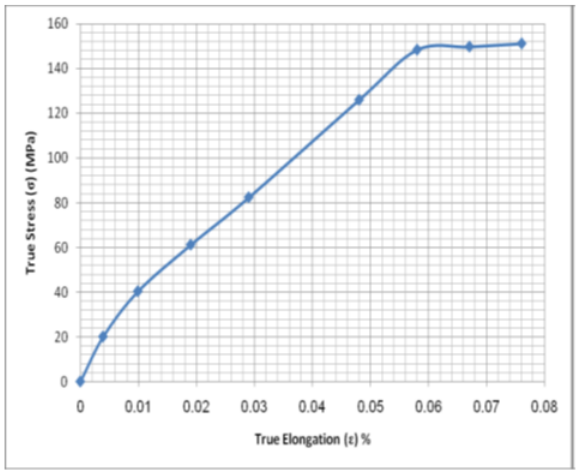

. Figure (9): Plot showing the relationship between true stress-strain.

Analysis and Discussion:

The results were discussed on several axes as follows:

1- Effect of Defect Size and Shape on Fracture: After forming the models containing the mentioned three types of defects (A&B&C) and shaping them with the press until the models fractured, the fracture depth from the center of the examined models was measured. The results obtained were compared with a defect-free model (intact piece). Table (1) shows the fracture depth from the center of three models, each containing one of the three types of defects, and compares them with a fourth intact model.

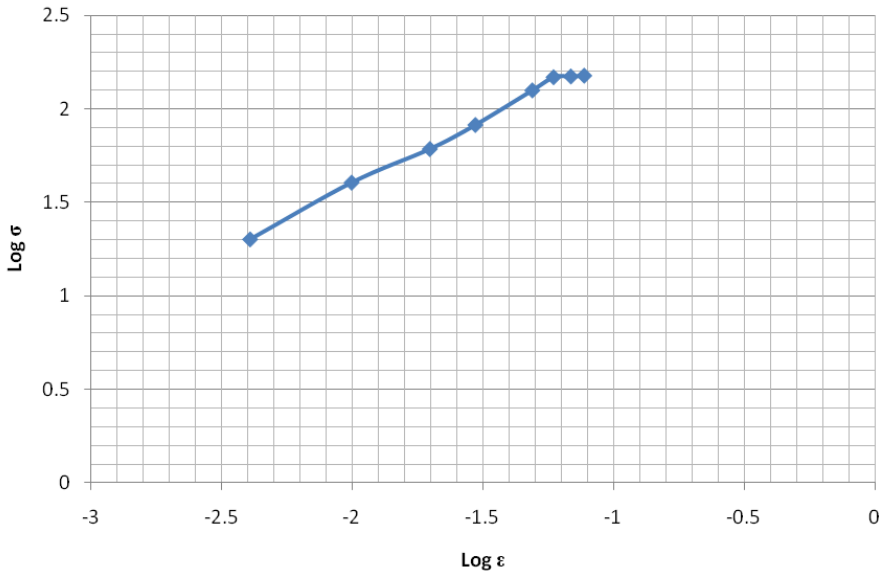

Figure (10): Plot showing the relationship between logarithmic true stress and logarithmic true strain.

Table (1): Fracture Depth from the Center of Three Models, Each Containing One of the Three Types of Defects, and Comparison with a Fourth Intact Model:

After Fracture from the Center of the Piece Containing Defect Type (C).	After Fracture from the Center of the Piece Containing Defect Type (B).	After Fracture from the Center of the Piece Containing Defect Type (A).	After Fracture from the Center of the Intact Piece.
8mm	*8.5mm*	*9mm*	*9mm*

From the tables, it is observed that the fracture depth from the center of the intact model is (9*mm*). In the case of twisting the model with a defect of type (A), the fracture depth from the center was (9 *mm*). In this case, there was no effect on the fracture depth from the center of the model, and the reason for this is that the defect size was relatively small (0.025 mm^3), smaller than the size of the other defects. As for the models containing defects of type (B&C) with larger sizes (2.235-1.047 mm^3), respectively, the effect was clear and stronger on the fracture region. The presence of defects led to the fracture creeping towards the center of the models. If defects were found, they would creep towards the center of the models, causing deformation in them instead of the previous area (in the intact model). Consequently, this led to the fracture creeping towards the center of the model. In some cases, significant distortion in the shape of defects was observed, especially defects with larger sizes, as shown in Figure (11). It is evident that the fracture area was close to the defect area, indicating that the larger the defect size, the greater its effect on initiating and propagating fracture. The effect of strain hardening caused by either cold forming or localized soft forming in those areas significantly contributed to the fracture process.

Figure (11): Models containing defects of large size.

As for the shape of the defect, researcher Henry pointed out the effect of the defect shape on fracture, stating that defects with sharp edges facilitate the initiation and propagation of fracture [7]. In the cases addressed in this study (A&B&C), defect type (A) contains somewhat sharp edges, represented by the conical value, while types (B&C) do not because they are hemispherical. However, the effect of defect size overshadowed the effect of defect shape, as the size of defects (B&C) is larger than that of defect (A). Due to the unavailability of cones in the hardness testing device using the (HRC) method with the ball size used in the (HRB) method and the inability to adjust the die size and the precision of defect creation manually, we could not prove the effect of sharp edges of the defect on fracture. However, based on the theory of racking and fracture, if all defects (A&B&C) were of the same size, the effect of defect type (A) on fracture would be greater than that of the other types.

2- Effect of Defect Location on Fracture: To investigate the effect of defect location on fracture, a relationship between fracture depth from the center of the tested models and the radius of the circle on which the defects were distributed was plotted. Figure (12) illustrates the effect of defect location distributed on circles of different diameters, represented by the symbol (O).

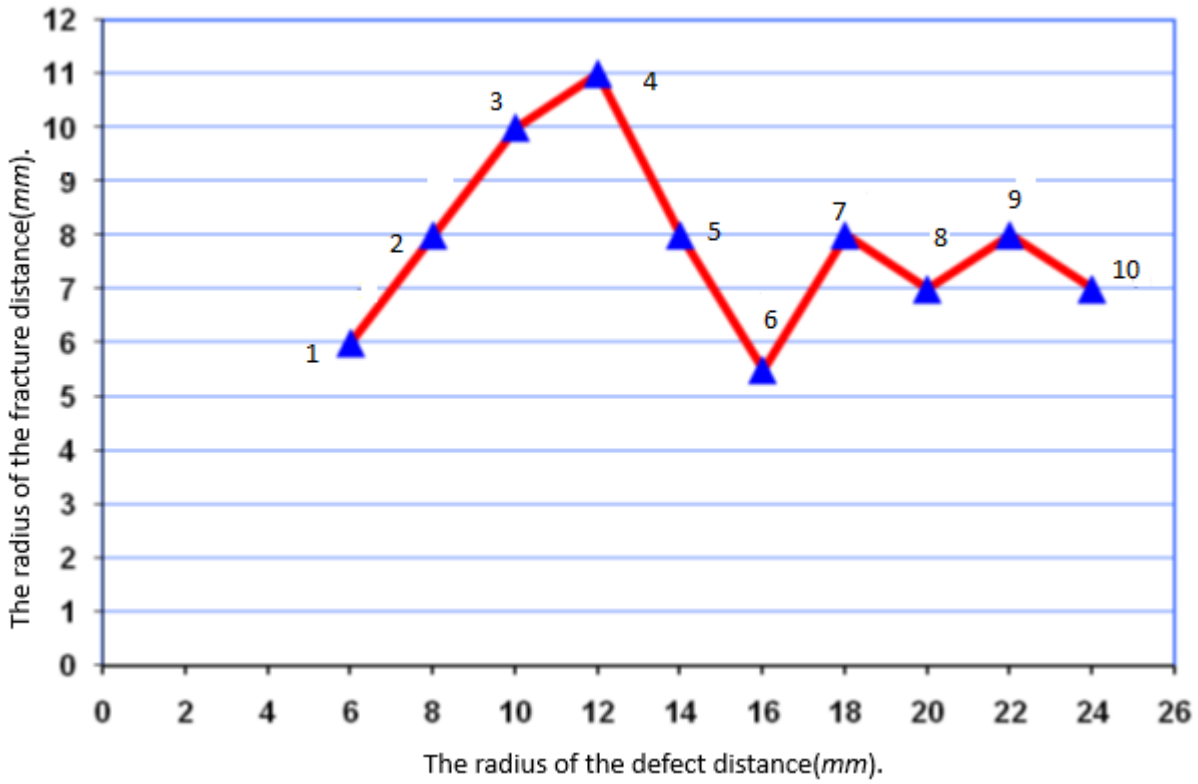

Fig(12)A diagram illustrating the relationship between the radius after fracture and the radius after the defect

From the figure, it is generally observed that changing the defect location has a significant impact on the fracture location. Comparing the results in the previous plot, it is noted that the fracture in most distribution areas was affected by the defect location, differing from its location in the intact model (as previously mentioned, the fracture radius for the intact piece was 9 *mm*). For example, at points (1-2-5-6-7-8-9-10), it is observed that the fracture radius is less than 9 mm, indicating that these defect distribution locations lead to fracture creeping towards the model to varying extents. Point (6) recorded a fracture radius of 5.5 mm, and likewise, point (1) recorded a fracture radius of 6 mm, indicating that these two locations have the greatest effect on fracture. As for points (10-8), a fracture radius of (7 *mm*) was recorded, indicating a lesser effect on fracture in these locations.

Regarding points (2-5-7-9), a fracture radius of (7 *mm*) was recorded, indicating the least effect on fracture. Points (3-4) caused the fracture to creep away from the center of the model, with fracture radii of 10-11 *mm*, respectively.

It is necessary to note that defect distribution started from a circle with a radius of 6 *mm*, as distribution on circles smaller than this did not affect the fracture location (indicating no formation in these areas), or there was minimal formation compared to other areas. Other areas affecting fracture can be classified into two types:

A. Areas causing the fracture to creep towards the center of the piece, representing 80% of the total models. In 10% of the models, the fracture crept towards the center by 3.5 mm from its original position, and in 10% of the models, the fracture crept towards the center by 3 *mm* from its original position. Additionally, in 20% of the models, the fracture crept towards the center by 2 *mm*, and in 40% of the models, the fracture crept towards the center by 1 *mm*.

B. Areas causing the fracture to creep away from the center of the piece, representing 20% of the total models. In 10% of the models, the fracture crept outside its original position by 1 *mm*, and likewise, in 10% of the models, the fracture crept outside by (2 *mm*.) Researchers Erik Schedin & Arne Melander indicated that stress distribution on the surface of the formed piece varies from one area to another and is usually concentrated towards the center of the piece in press forming operations[8]. This was clearly evident from the previous results, where the presence of defects and the occurrence of strain hardening caused by defects in some areas resulted in the fracture creeping towards the center of the formed piece, accounting for 80% of the results, explaining the reason for the fracture creep

Effect of Defect Distribution Methods on Fracture

From Figure (13) and upon comparing the first distribution of defects, which were distributed along the perimeters of circles of various diameters, denoted by symbol (O), with the other distribution, which was along perpendicular diameters, denoted by symbol (X), we can easily observe the significant impact of defect distribution along the circles (O) on the fracture location compared to the distribution along perpendicular diameters. In the first distribution type, there was a two-way effect, as previously mentioned in (A&B).

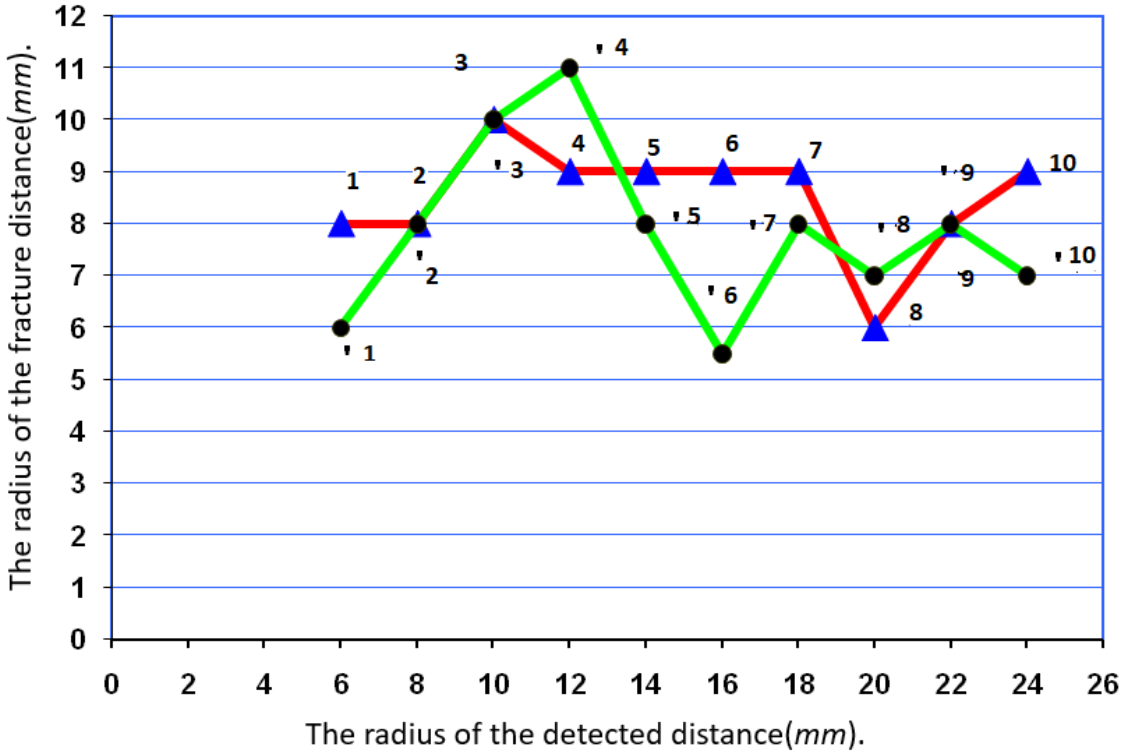

Figure (13): A diagram comparing distributions (X) & (O).

As for the second distribution, it is observed that the impact is divided into:

1- Creep of the fracture towards the center, as seen at points (1□-2□-8□-9□), representing 40% of the models.

2- Creep of the fracture away from the center of the piece, as seen at point (3□), representing 10% of the models.

3- Appearance of the fracture at a distance of 9 *mm* from the center, as seen at points (4□-5□-6□-7□-10□), which is half the fracture radius of the intact piece.

The fracture location was not affected, representing the prevailing effect of this distribution, accounting for 50% of the models.

It should be noted that points (2-2′) had a similar effect in both distributions (causing the fracture to creep towards the center), but it had a greater effect in the first distribution, where this point represented 40% of the first distribution and 30% of the second distribution. Similarly, section (3-3□) in both distributions had the same effect. The same applies to (9□-9). From the aforementioned, we can conclude that the first distribution had a greater effect on the fracture location compared to the second distribution, which had very little effect. In the second distribution, 50% of the distribution areas did not affect the fracture location, and the remaining areas had a minimal effect, causing a creep of only 1 *mm* in most cases. As for the first distribution, all models affected the fracture location, as no piece from distribution (O) remained intact, resulting in a fracture at a distance of 9 *mm*, which is the fracture depth from the center in the intact piece. This percentage is illustrated in the cumulative histogram in Figure (14).

This can be explained by the fact that in the second distribution, with the gathering of diameters, there was a group of defects located at a distance of 9 mm from the center (which is the

fracture radius of the intact model). Thus, all pieces in this distribution type contained defects in the expected fracture area before the forming process, leading to fracture in that area. As for the explanation of the appearance of fractures in areas far from the defects, it can be attributed to the difference in stress distribution on the surface of the formed piece, as indicated by researchers Erik Schedin & Arne Malander, where the presence of defects in some areas led to a change in stress distribution, concentrating it in those areas instead of the expected fracture area. This can also be explained by the fact that in the case of distribution (X), the number of defects was less for each piece and they were distributed across diameters of different sizes within the piece. This type of defect distribution affected the fracture location relative to its original location in the intact piece (9 *mm*).

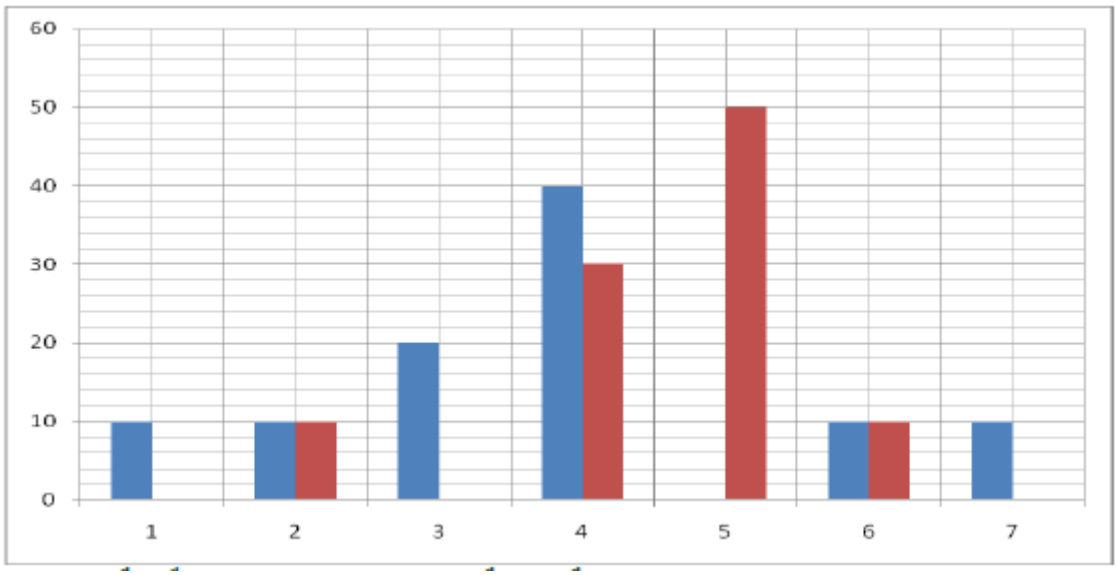

Figure (14) is a cumulative histogram showing the percentage of creep of the fracture away from the center of the piece.

IV. Conclusions:

The larger the defect, the greater its effect on forming.

Fracture process in the case of distribution type (O) is irregular, either occurring far or close to the fracture center (9 *mm*).

It was observed from the tests that in distribution type (X), most fracture areas were at 9 *mm*, which is the same as the intact piece.

References:

[1]. Journal of Atomic World (Syrian Electricity Authority Magazine), Issue 112 (October) for the year 2007.
[2]. Principles of Metal and Material Engineering by Dr. Hussein Baqir, Mosul University, 1985.
[3]. Formability Characteristics of Aluminum Sheet . K. Sieger and S. Wanger Stuttgart University.1994.
[4]. Amp Journal Technology Vol.5 \ June 1996.
[5]. The Science and Engineering of Materials .Donald R Askeland 2004.
[6]. Metal forming, fundamental and applications American society for metals 1985 Forming and Forging Vol. 14 1993.
[7]. Deformable Bodies and their Material Behavior . Henry W. Has Lach, JR.2004.
[8]. On the Strain Distribution During the Stretch Forming of Low and Hidh Strength Sheet Steel. Erik Schedin and Arne Melander ,Journal of Mechanical working Technology vol.15 1087.